Piecewise affine control for fast unmanned ground vehicles

André Benine-Neto, Christophe Grand

Piecewise Affine Control for Fast Unmanned Ground Vehicles

André Benine-Neto[1] and Christophe Grand[1]

Abstract— **Unmanned ground vehicles (UGV) may experience skidding when moving at high speeds, and therefore have its safety jeopardized. For this reason the nonlinear dynamics of lateral tire forces must be taken into account into the design of steering controllers for autonomous vehicles. This paper presents the design of a state feedback piecewise affine controller applied to an UGV to coordinate the steering and torque distribution inputs in order to reduce vehicle skidding on demanding maneuvers. The control synthesis consists in solving an optimization procedure involving constraints in the form of Linear Matrix Inequalities which are obtained from stability conditions of a piecewise quadratic Lyapunov function. The improved performance of the piecewise affine controller with respect to a linear controller is confirmed through simulations on degraded tire-floor adhesion.**

I. INTRODUCTION

Increasingly attention and research has been recently devoted to the development unmanned ground vehicles (UGV) at high speeds, mainly motivated by applications such as transportation, search and rescue, surveillance and disaster relief. Faster displacement is advantageous in several autonomous tasks, which may become more effective if accomplished in less time [1]. Vehicle dynamic effects such as rollover, ballistic motion, sideslip and wheelslip may occur at high speeds, specially on degraded surfaces due low adhesion or roughness. Therefore these aspects must be treated adequately in order to ensure the safety of the vehicle and satisfactory performance of the planned maneuvers as in [1] and [2] considering vehicle control on rough ground and on loose surfaces, respectively .

Usually the inputs for controlling the lateral dynamics of UGV consist of wheel steering, but independent wheel traction can also be used to generate yaw moment. Combined actions of both control inputs is also subject of recent research [3], [4].

In order to design controller for UGV which are able to operate at high speeds which involve large vehicle sideslip, the nonlinear behavior of the lateral tire forces may not be neglected. Piecewise affine (PWA) systems are able to capture saturations of engineering systems and also approximate nonlinearities arbitrarily [5], being thus an interesting approach for the design of controllers for nonlinear system (*e.g.* [5], [6], [7]). Concerning vehicle lateral control, some applications of PWA controllers can be found in [8] and [9], respectively for the design of vehicle handling and path following systems.

[1]A. Benine-Neto and C. Grand are with Institut des Systèmes Intelligents et de Robotique (ISIR), Université Pierre et Marie Curie, 4 Place Jussieu, 75005 Paris, France {benine-neto, grand} @isir.upmc.fr

This paper addresses the design of a PWA state feedback controller for a path following application of a four-wheel UGV, which is capable of handling vehicle instability by avoiding skidding at the slipping behavior of tire forces. The UGV is equipped with front wheel steering system and independent propulsion torque at each wheel, that allows the generation of yaw moments. The proposed PWA controller can be considered as an extension of linear state feedback from [3], since it takes into account the nonlinear behavior of lateral tire forces. The control synthesis of the proposed PWA controller is based on the search of a Piecewise Quadratic Lyapunov (PWQL) function by means of optimization procedure involving Linear Matrix Inequalities constraints (LMI) [7].

The paper is organized as follows: the next section shows development of PWA model used in the control synthesis, developed from a commonly used single track nonlinear model. In addition, assumptions required for the proposed control synthesis are also discussed. Section III is dedicated to the the control PWA control strategy, presenting the LMI constraints used in the convex optimization process for control synthesis, as well as proposal for the repartition of the control efforts. In section IV, the numerical results from the control synthesis are presented. Then, resulting performance is analyzed from simulations using a nonlinear model of UGV with degraded tire-ground adhesion. The conclusions and perspectives in section V wrap up the paper.

II. FAST ROBOT MODEL

A widely used simplified single track vehicle model [10], which is considered to capture the essential vehicle lateral steering dynamics, is approximated by a PWA system in order to design the controllers that avoid saturation of the lateral tire forces.

A. Nonlinear Vehicle Model

The wheels of the front and rear axles are lumped into one located at the axle center, and only the lateral translational and yaw motions are considered while the roll and pitch motions are neglected. The dynamic equations describing this model are given by:

$$\begin{cases} m(\dot{v}_y + rv_x) = F_{yf}\cos\delta_f + F_{yr} \\ J\dot{r} = l_f F_{yf}\cos\delta_f - l_r F_{yr} + M_z, \end{cases} \quad (1)$$

where v_x and v_y are the lateral and longitudinal vehicle speed, r is the vehicle yaw rate, δ_f is the steering angle, m is the vehicle mass, l_f and l_r are the distances from the front and rear axle, respectively, to the center of gravity (CG), J is the vehicle inertia respect to the vertical axle through

the CG, M_z is the resulting yaw moment from differential torque, F_{yf} and F_{yr} are the front and rear lateral forces, which are represented according to Pacejka's model [11] as follows:

$$F_{y\kappa}(\alpha_\kappa) = D_\kappa \sin(C_\kappa \mathrm{atan}[(1-E_\kappa)B_\kappa\alpha_\kappa + E_\kappa \mathrm{atan}(B_\kappa\alpha_\kappa)]), \tag{2}$$

where α_κ, with $\kappa = (f, r)$, stands for the front or rear tire sideslip angle. Considering that the angles remain small, the sideslip angles for front and rear tires are given by:

$$\alpha_f = \delta_f - \beta - l_f r/v, \qquad \alpha_r = -\beta + l_r r/v, \tag{3}$$

where β is the vehicle sideslip angle, which replaces v_y since $v_y = v_x \sin\beta$, and the approximation $v = v_x$ is also valid.

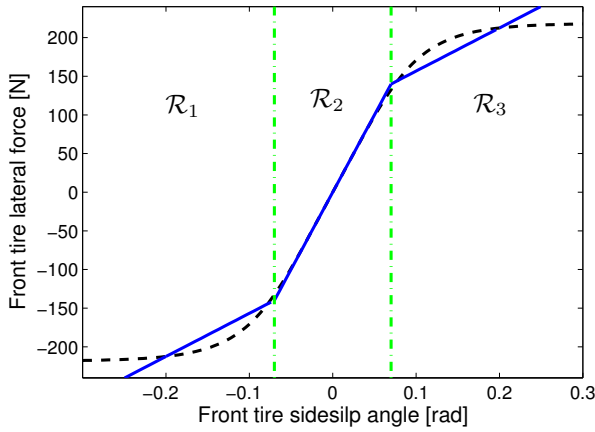The black dashed curve in Fig. 1 illustrates the Pacejka model for the front wheel.

Fig. 1. Pacejka model for front wheel lateral tire force (dashed) and PWA approximations (solid), according to partitioning of wheel sideslip angle domain (dash-dot) in three operating regions.

In order to include the positioning of the UGV with respect to a predefined path, the model (1) has to be expanded with the dynamics of the relative yaw angle and the lateral displacement with respect to the path center-line. Let $\psi_L = \psi - \psi_d$ be the yaw angle error which is the angle between the vehicle orientation and the tangent to the road. The path reference curvature ρ_{ref} is defined by ($\dot{\psi}_d = v\rho_{ref}$), and the following equality can be derived:

$$\dot{\psi}_L = r - v\rho_{ref}. \tag{4}$$

Denoting by l_s the look-ahead distance, the equation giving the dynamics of the measurement of the lateral offset y_L from the center-line is obtained by

$$\dot{y}_L = v(\beta + \psi_L) + l_s r. \tag{5}$$

An illustration of the state variables is provided in Fig. 2, and the numerical values of the vehicle parameters are presented in Table I.

B. PWA Model for Lateral Dynamics

In order to take into account the nonlinear behavior of the lateral tire forces, the Pacejka tire model (2) can be approximated by the following PWA functions:

$$F_{y\kappa} = d_{\kappa i}\alpha_\kappa + e_{\kappa i}, \text{ if } \alpha_\kappa \in \mathcal{R}_i \tag{6}$$
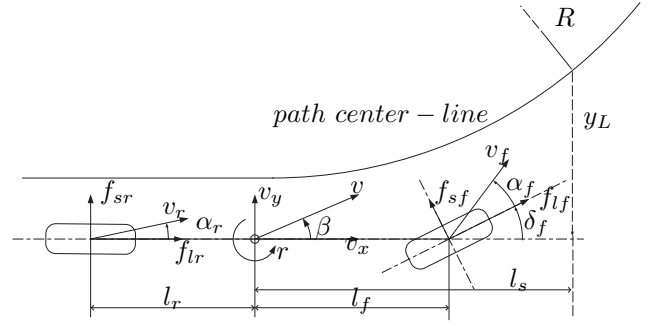

Fig. 2. Single track vehicle model.

with $\kappa = (f, r)$, and the index i representing the polytopic operating region $\mathcal{R}_i$ which are defined by intervals of the front and rear tire sideslip angles, *i.e.* $\mathcal{R}_i = [\underline{\alpha}_{ri}\bar{\alpha}_{ri}) \cap [\underline{\alpha}_{fi}\bar{\alpha}_{fi})$, with $\underline{\alpha}_{\kappa i}$ and $\bar{\alpha}_{\kappa i}$ being the lower and upper bounds of intervals, respectively. The blue lines in Fig. 1 illustrate PWA approximations for the front tire.

According to (3), the boundaries of operating regions expressed in terms of the front wheel sideslip angle are directly affected by the steering angle. Such situation should be avoided in order to employ the control synthesis based on PWQL functions, therefore it is preferable to express the partitions of the operating regions in term of state variables. As suggested in [6] and [7], a first-order dynamics, with large enough bandwidth, representing the steering actuator is included in the vehicle model:

$$\dot{\delta}_f = -\omega_0\delta_f + \omega_0 u_c, \tag{7}$$

where $\omega_0 = 62.8 rad/s$, and $u = [u_c, \ M_z]^T$ becomes the new control input.

To obtain a PWA model of the UGV, (1) is linearized about uniform rectilinear motion and the nonlinear lateral tire forces are replaced by the PWA approximations (6). Equations (5) and (4) representing the positioning with respect to the center of the planned path and (7) representing the actuator dynamics are included, leading to the following PWA system:

$$\dot{x} = A_i x + B_i u + B_\rho \rho_{pref} + a_i \tag{8}$$

where $x = [\beta, r, \psi_L, y_L, \delta_f]^T$, $u = [u_c, \ M_z]^T$ and the corresponding dynamics are:

$$A_i = \begin{bmatrix} -2\frac{d_{fi}+d_{ri}}{mv} & -1-2\frac{d_{fi}l_f - d_{ri}l_r}{mv^2} & 0 & 0 & \frac{2d_{fi}}{mv} \\ 2\frac{d_{ri}l_r - d_{fi}l_f}{J} & -2\frac{d_{fi}l_f^2 + d_{ri}l_r^2}{Jv} & 0 & 0 & \frac{2d_{fi}l_f}{J} \\ 0 & 1 & 0 & 0 & 0 \\ v & l_s & v & 0 & 0 \\ 0 & 0 & 0 & 0 & -\omega_0 \end{bmatrix},$$

$$B_i = \begin{bmatrix} 0 & 0 \\ 0 & \frac{1}{J} \\ 0 & 0 \\ 0 & 0 \\ \omega_0 & 0 \end{bmatrix}, \quad B_\rho = \begin{bmatrix} 0 \\ 0 \\ -v \\ 0 \\ 0 \end{bmatrix}, \quad a_i = \begin{bmatrix} 2\frac{e_{fi}+e_{ri}}{mv} \\ 2\frac{e_{fi}l_f - e_{ri}l_r}{Jv} \\ 0 \\ 0 \\ 0 \end{bmatrix}. \tag{9}$$

The operating regions $\mathcal{R}_i$ can be then described in terms of state space variables, as follows:

$$\mathcal{R}_i = \left\{ x \in \mathbb{R}^5 \ / \ H_i x - g_i < 0 \right\} \tag{10}$$

where

$$H_i = \begin{bmatrix} -1 & -l_f/v & 0 & 0 & 1 \\ 1 & l_f/v & 0 & 0 & -1 \\ -1 & l_r/v & 0 & 0 & 0 \\ 1 & -l_r/v & 0 & 0 & 0 \end{bmatrix}, \ g_i = \begin{bmatrix} -\bar{\alpha}_{fi}, \\ \underline{\alpha}_{fi}, \\ -\bar{\alpha}_{ri}, \\ \underline{\alpha}_{ri} \end{bmatrix}. \tag{11}$$

C. Assumptions for PWA Control Synthesis

It is considered that the vehicle has understeering behavior, therefore, only the nonlinear behavior of the front tire is taken into account. For the rear tire, a simple linear approximation is considered for the whole domain of wheel sideslip angle, *i.e.* d_{ri} is constant and $e_{ri} = 0$. An analogous approach may be employed for oversteering vehicles.

This simplification renders the operating regions slab, so that they can be exactly described by degenerated ellipsoids [6], [7], as follows:

$$\mathcal{R}_i = \left\{ x \in \mathbb{R}^5 \ / \ ||E_i x + f_i||_2 \leq 1 \right\} \tag{12}$$

where, $E_i = \frac{2}{\bar{\alpha}_{fi} - \underline{\alpha}_{fi}}[-1, \ -l_f/v, \ 0, \ 0, \ -1]$ and $f_i = -\frac{\bar{\alpha}_{fi} + \underline{\alpha}_{fi}}{\bar{\alpha}_{fi} - \underline{\alpha}_{fi}}$.

Such representation is advantageous in comparison to (10) since it yields the search of less unknowns during the optimization procedure, as it is shown in section III. Moreover, only three regions are considered in the PWA model for the control synthesis in order to reduce the number of constraints. The regions are delimited by symmetrical threshold values $\alpha_f = \pm \bar{\alpha}_f$ as shown in Fig. 1. Although PWA system may approximate the nonlinearities to arbitrarily precision, the results obtained with this simple approximation can already enhance the performance as it will be shown in section IV.

Disturbances and exogenous inputs, such as the planned path curvature, are not taken into account for the control synthesis, therefore ρ_{ref} is set to zero in the model describing the vehicle dynamics (8).

All the state variables are supposed available for measurement. Although sophisticated algorithms exist for the estimation of the front wheel sideslip angle, such as [12], in the proposed approach this variable is computed according to (3) due to its simplicity in implementation.

It is assumed that a lower level controller acting on the propulsion torque of each wheel is able to adequately generate the yaw moment M_z.

III. CONTROL STRATEGY

The procedure proposed in [7] is used to compute the PWA controllers for the UGV. The goal is to stabilize the PWA vehicle model (8), with a PWA state feedback gain $u = K_i x + m_i$. The closed-loop state-space equation becomes:

$$\dot{x} = (A_i + B_i K_i)x + (a_i + B_i m_i) = \bar{A}_i x + \bar{b}_i. \tag{13}$$

The matrix $\bar{A}_i$ of the closed loop system of each region is designed such that it is invertible and its equilibrium point is denoted x_{eq}^i. This condition is mathematically expressed by:

$$(A_i + B_i K_i)x_{eq}^i + (a_i + B_i m_i) = 0. \tag{14}$$

A. Piecewise Quadratic Lyapunov Based Control

The asymptotic stability of the closed-loop system (13) can be ensured by the existence of a PWQL function. Such form is less conservative than a single quadratic Lyapunov function and it can be written as:

$$V_i(x) = x^T P_i x + 2q_i^T x + r_i, \tag{15}$$

where $P_i = P_i^T$ and for this application, $P_i \in \mathbb{R}^{5 \times 5}$, $q_i \in \mathbb{R}^5$, and $r_i \in \mathbb{R}$. $V_i(x)$ is a Lyapunov function with a decay rate α_i, for the region $\mathcal{R}_i$ if the following conditions are satisfied:

$$x \in \mathcal{R}_i, \begin{cases} V_i(x) > \epsilon ||x - x_{eq}||_2 \\ \frac{d}{dt}V_i(x) < -\alpha_i V_i(x), \end{cases} \tag{16}$$

where x_{eq} is the equilibrium point of the closed loop system and $\epsilon \geq 0$ is a fixed constant.

Since the lateral tire forces are symmetric with respect to the origin, as well as the dynamics of the PWA vehicle model (8), only regions $\mathcal{R}_1$ and $\mathcal{R}_2$ are considered in the control synthesis. The gains obtained for region $\mathcal{R}_1$ can be applied in region $\mathcal{R}_3$, *e.g.* $K_1 = K_3$ and $m_1 = -m_3$. This simplification reduces the number of LMIs to be solved.

Rendering the vehicle to the center of the planned path is a stabilization problem for systems (13), since in a straight line all state variables should converge to the origin. Therefore the desired equilibrium point of the closed loop system, x_{eq} is placed at the origin. Since $x_{eq} \in \mathcal{R}_2$, the terms of the PWQL function (15) are then set to $q_2 = 0_{5 \times 1}$ and $r_2 = 0$ to ensure that $V(0) = 0$ for systems (13). Consequently, the Lyapunov stability condition (16) relative to $\mathcal{R}_2$ can simply be rewritten in LMI form as for a linear system:

$$\begin{cases} \begin{bmatrix} P_2 - \epsilon I_n \end{bmatrix} \succ 0 \\ \begin{bmatrix} \bar{A}_2^T P_2 + P_2 \bar{A}_2 + \alpha_2 P_2 \end{bmatrix} \prec 0 \end{cases} \tag{17}$$

Concerning the dynamics in $\mathcal{R}_1$, there is no need to impose conditions (16) to the whole state space, since they must be valid only in $\mathcal{R}_1$. These conditions may be relaxed by the use of S-Procedure [13], due to the quadratic form of the ellipsoidal description for the operating regions (12), as follows:

$$\begin{cases} \lambda_1 > 0, \ \gamma_1 > 0, \\ \begin{bmatrix} P_1 - \epsilon I_n + \lambda_1 E_1^T E_1 & q_1 + \epsilon x_{eq} + \lambda_1 E_1^T f_1 \\ & r_i - \epsilon x_{eq}^T x_{eq} \\ * & +\lambda_1(f_1^T f_1 - 1) \end{bmatrix} \succ 0 \\ \begin{bmatrix} \bar{A}_1^T P_1 + P_1 \bar{A}_1 & P_1 \bar{b}_1 + \bar{A}_1^T q_1 \\ -\gamma_1 E_1^T E_1 + \alpha_1 P_1 & +\alpha_1 q_1 - \gamma_1 E_1^T f_1 \\ & 2\bar{b}_1^T q_1 + \alpha_1 r_1 \\ * & -\gamma_1(f_1^T f_1 - 1) \end{bmatrix} \prec 0 \end{cases} \tag{18}$$

where λ_1 and γ_1 are scalars and $*$ indicates the transpose.

The continuity of the PQWL function (15) across the borders of $\mathcal{R}_1$ and $\mathcal{R}_2$ is ensured by the following constraint:

$$\begin{cases} F_{\{1,2\}}^T(P_1 - P_2)F_{\{1,2\}} = 0 \\ F_{\{1,2\}}^T(P_1 - P_2)l_{\{1,2\}} + F_{\{1,2\}}^T(q_1) = 0 \\ l_{\{1,2\}}^T(P_1 - P_2)l_{\{1,2\}} + 2(q_1)^T l_{\{1,2\}} + (r_1) = 0 \end{cases}$$

(19)

where:

$$F_{\{1,2\}} = \begin{bmatrix} -\frac{l_f}{v} & 0 & 0 & 1 \\ 1 & 0 & 0 & 0 \\ 0 & 1 & 0 & 0 \\ 0 & 0 & 1 & 0 \\ 0 & 0 & 0 & 1 \end{bmatrix}, \; l_{\{1,2\}} = \begin{bmatrix} \frac{\bar{\alpha}_f}{2+l_f^2/v^2} \\ \frac{\bar{\alpha}_f l_f}{v(2+l_f^2/v^2)} \\ 0 \\ 0 \\ \frac{-\bar{\alpha}_f}{2+l_f^2/v^2} \end{bmatrix},$$

(20)

obtained from a parametric description of the cell boundaries, as a subset of the state space (see [6], [7]), given by: $\bar{\mathcal{R}}_1 \cap \bar{\mathcal{R}}_2 \subseteq \{l_{\{1,2\}} + F_{\{1,2\}}s \; / \; s \in \mathbb{R}^4\}$. The elements of (20) are computed considering $\mathcal{H}_{\{1,2\}} = \left\{x \; / \; h_{\{1,2\}}^T x + \bar{\alpha}_f = 0\right\}$ the hyperplane in which the facet boundary between the regions $\mathcal{R}_1$ and $\mathcal{R}_2$ is contained, hence $h_{\{1,2\}}^T = [-1, \; -l_f/v, \; 0, \; 0, \; 1]$. Then, $F_{\{1,2\}} \in \mathbb{R}^{5 \times 4}$ (full rank) is the matrix whose columns span the null space of $h_{\{1,2\}}$, and $l_{\{1,2\}} \in \mathbb{R}^5$ is given by $l_{\{1,2\}} = -h_{\{1,2\}}(h_{\{1,2\}}^T h_{\{1,2\}})^{-1}\bar{\alpha}_f$.

Constraints (18) consist of a Bilinear Matrix Inequality (BMI) due to the product of P_1 and B_1K_1. Although algorithms are available for solving BMI (*i.g.* [14]), the V-K iterative method [7] was used in this work. This algorithm consists in solving alternately two LMI problems which are obtained by fixing one of the terms in the BMI, as follows:

V-step: Given a fixed controller, and fixed decay rates α_i, solve:

$$\text{Find: } P_1, \; q_1, \; r_1 \text{ and } P_2,$$

$$\text{such that: (17), (18), (19),}$$

$$\epsilon > 0, \quad \gamma_1 > 0, \quad \lambda_1 > 0,$$

(21)

K-step: For P_i, q_i and r_i fixed at the previous step, solve:

$$\max\left(\min_i \alpha_i\right)$$

$$\text{such that (14), (18), (17),}$$

$$\epsilon > 0, \quad \gamma_1 > 0, \quad \lambda_1 > 0, \quad \alpha_i > l_0 > 0,$$

$$-l_1 < K_i < l_1, \quad -l_2 < m_i < l_2,$$

(22)

where l_1 and l_2 are vector bounds.

For each iteration of the K-step, the decay rates α_1 and α_2 must be greater than the value computed at the previous iteration. The loop must be repeated until there is no significant improvement on the cost function or the LMIs become infeasible. The previously obtained results are thus retained.

B. Repartition of Control efforts

The repartition of the control inputs (steering and yaw moment) is moderated by two parameters, $\mu_{\delta_f} \in [\mu_{\delta_f}^{min}, \mu_{\delta_f}^{max}]$ and $\mu_T \in [\mu_T^{min}, \mu_T^{max}]$. These parameters depend on the front wheel sideslip angle, following the gaussian functions:

$$\mu_{\delta_f} = \mu_{\delta_f}^{min} + (\mu_{\delta_f}^{max} - \mu_{\delta_f}^{min})e^{-\alpha_f^2/2\sigma_{\delta_f}^2}$$
$$\mu_T = 1 - \left(\mu_T^{min} + (\mu_T^{max} - \mu_T^{min})e^{-\alpha_f^2/2\sigma_T^2}\right)$$

(23)

where σ_{δ_f} and σ_T are calibration parameters that influences their dispersion. Such strategy privileges the use of steering angle in the linear domain of tire forces, and tends to increase the contribution of differential torque as the lateral tire forces tend to saturate. The repartition of the control efforts is taken into account in the control synthesis of the initial controller, so that the closed-loop system is asymptotically stable with any combination of μ_{δ_f} and μ_T, as detailed in the subsequent section.

IV. RESULTS

In this section the initial controller and iterations of the V-K method (21)-(22) are presented, as well as the simulation results obtained with the synthesized PWA controller.

A. PWA state feedback control synthesis

The choice of an initial controller, $K_i^{k=0}$, used in the first iteration the V-K method is important for the proposed PWA control synthesis. Several possibilities exist in the literature, including LQR, as presented in [7]. In this paper, the initial controllers are obtained from the control synthesis proposed in [3]. Such approach is particularly interesting, since it employs quadratic Lyapunov stability condition and LMI methods for the computation of a linear state feedback controller in the design of a driver assistance system with steering and differential braking as control inputs. In order to compute the gains for the initial controller, a linear vehicle model has been used. For that, only the dynamics of $\mathcal{R}_2$ from (8) are considered. The vehicle parameters involved in the control synthesis from [3] are shown in Table I. The computed gain

$$K_i^{k=0} = \begin{bmatrix} 0.006, & -0.069, & -0.318, & -0.027, & -0.044 \\ 3.077, & -15.201, & -30.865, & -2.352, & 0.712 \end{bmatrix},$$

(24)

has been applied for $\mathcal{R}_1$ and $\mathcal{R}_2$ at the first iteration, with m_i being set to zero for both regions.

The V-K method tends to generate controllers that are too reactive, due to the maximization of the decay rates in the objective function. Although the limitations of the actuators have been taken into account for the synthesis of (24) using the procedure from [3], the same constraints cannot be used in the V-K method, since the they would require the computation of P_i^{-1}, and consequently another parametrisation of the boundaries to ensure the continuity of the PWQL function (19). In order to circumvent this adversity, the controller corresponding to the linear region is

limited to a fixed range of the initial controller through the following constraint added to the K-Step of the algorithm:

$$0.7|K_i^0| < |K_2^k| < 1.3|K_i^0| \tag{25}$$

Each step of the V-K method has been solved using [15]. Considering (24) as initial controller, $\epsilon = 10^{-6}$, $l_1 = 2|K_i^0|$, $l_2 = [\delta_f^{max}, \ M_z^{max}]^T$, a constant vehicle longitudinal speed $v = 10 \ m/s$ and the vehicle parameters as shown in Table I, The obtained gains are given by:

$$K_1 = \begin{bmatrix} -0.016 & -0.046 & -0.261 & -0.024 & 0.084 \\ 0.326 & 4.519 & -50.042 & 2.727 & 0.004 \end{bmatrix},$$

$$K_2 = \begin{bmatrix} 0.012 & -0.045 & -0.260 & -0.024 & 0.056 \\ 0.542 & 2.412 & 21.294 & 0.483 & 0.140 \end{bmatrix},$$

$$K_3 = K_1,$$

$$m_1 = \begin{bmatrix} 0.0025 \\ 32.5019 \end{bmatrix}, \ m_2 = \begin{bmatrix} 0 \\ 0 \end{bmatrix} \text{ and } m_3 = -m_1 \tag{26}$$

This resulting PWA controller has been implemented in a robot model for simulations as detailed in the subsequence.

B. Simulation Results

In order to evaluate the improvement of the PWA controller, the same maneuver has been performed with UGV in two configuration: UGV named *lin-crtl* is equipped with a linear controller corresponding to K_2; UGV named *PWA-crtl* is equipped with the PWA controller (26).

The maneuver consists of a left turn of 70° with fillet radius of $10m$. The vehicle longitudinal speed has been regulated by a proportional controller at $v = 10m/s$. For the simulations, a nonlinear four-wheel vehicle model has been used. The longitudinal and lateral forces of each tire are computed according to Pacejka model (2). The adhesion between the tires and the surface was allowed to vary randomly within the interval $\mu \in [0.7, \ 1]$ throughout the simulation. This condition is incorporated in the parameters of (2) by changing B_κ to $(2 - \mu)B_\kappa$, C_κ to $(5 - \mu)C_\kappa/4$ and D_κ to μD_κ, as detailed in [16].

The performance of both vehicles are depicted in Fig. 3-6, being *lin-crtl* represented by the dashed blue lines and the response of *PWA-crtl* is shown in solid black lines.

The planned path for the vehicle is shown in black thin dashed line on Fig 3. Since the maneuver is very demanding, the trajectories of both vehicles deviates from the reference. Nevertheless it is clear that the response of *PWA-crtl* in terms of positioning is improved, since it oscillates less than *lin-crtl*.

The dynamics of both vehicles during the maneuver is shown in Fig. 4. It can be seen that the PWA controller can significantly reduce the vehicle skidding by comparing both vehicles sideslip angles as depicted on the upper subplot. While $max(|\beta|)$ reaches $0.25 \ rad$ for *lin-crtl* it does not overcome $0.12 \ rad$ for *PWA-crtl*. The yaw rate of both vehicles are represented in the lower subplot of Fig. 4.

The steering angle is shown in the upper subplot of Fig. 5, and the lower subplot shows the computed front wheel sideslip angle, according to (3). It can be noticed that for
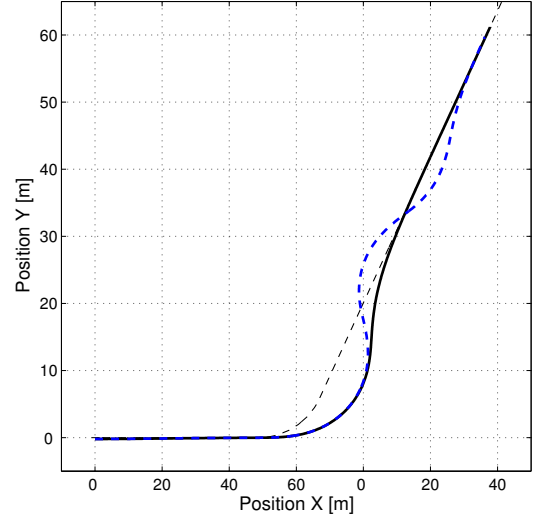

Fig. 3. Vehicle trajectories for *lin-crtl* in dashed blue line and *PWA-crtl* in solid black line
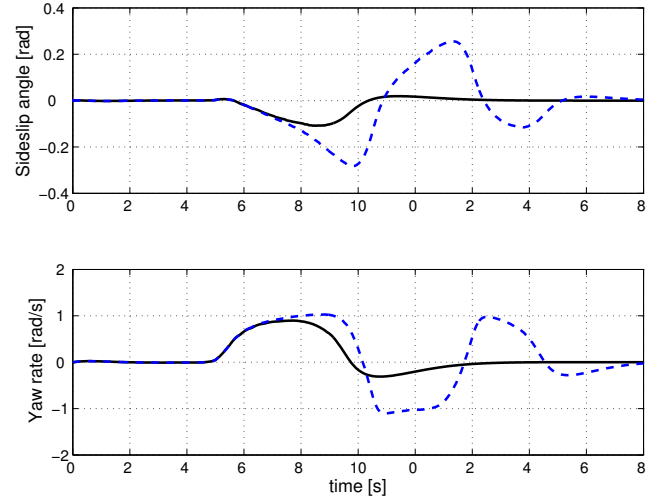

Fig. 4. Vehicle sideslip angle and yaw rate responses during maneuver for *lin-crtl* in dashed blue line and *PWA-crtl* in solid black line

both vehicles the front wheel sideslip angle surpasses the threshold delimiting the linear region, which induces the switching of the PWA controllers (from K_2 to K_3) for *PWA-crtl*. Due to the distinct input control, *PWA-crtl* operates in the sliding behavior of the tire forces over a shorter time interval when compared to the response of *lin-crtl*.

The control inputs u_c and M_z are shown respectively on the upper and lower subplots of Fig. 6.

V. CONCLUSIONS

In this paper the design of a PWA state feedback controller for lateral motion of a fast UGV has been presented. The controller is able to handle the sliding behavior of lateral tire forces, reducing the vehicle skidding by coordinated action of front wheel steering angle and four wheel independent torque distribution. For the PWA controller synthesis, a PWA modeling of the vehicle dynamics has been developed. In addition, a linear state feedback controller has been extended
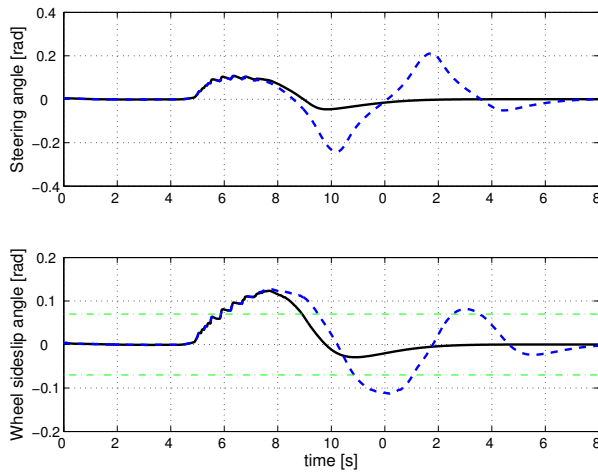
Fig. 5. Steering angle and front wheel sideslip angle during maneuver for *lin-crtl* in dashed blue line and *PWA-crtl* in solid black line
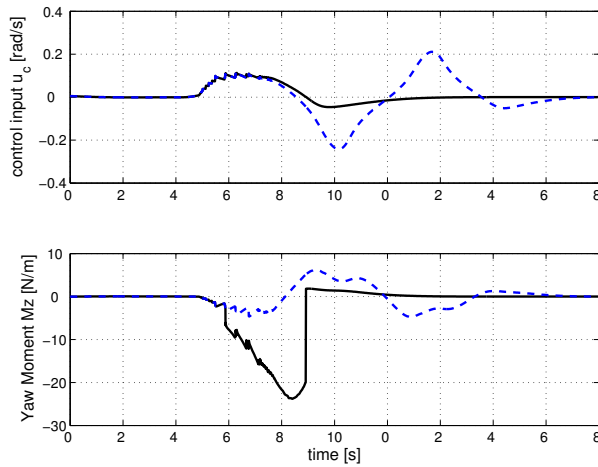

Fig. 6. Control inputs during maneuver for *lin-crtl* in dashed blue line and *PWA-crtl* in solid black line

to the PWA formulation by means of an optimization procedure under LMI constraints. The closed loop asymptotic stability is guaranteed by a PWQL function obtained from the solution of the same optimization problem. The improved performance of the PWA controller with respect to a controller considering only the linear region has been confirmed through simulation on a nonlinear UGV model with degraded tire-ground adhesion.

One of the main limitations of the proposed approach is the overshoot with respect to the desired path which may the be reduced considering anticipation algorithms or integration of a longitudinal dynamics control in order regulate the vehicle speed adequately according to the curvature. Future work should be focused on these aspects.

TABLE I
VEHICLE PARAMETERS AND PWA APPROXIMATIONS OF LATERAL TIRE FORCES

Vehicle Parameters			PWA approximations		
m	85	[kg]	d_{f1}	558	[N/rad]
J	58	[kg m^2]	d_{f2}	1999.8	[N/rad]
l_f	0.6	[m]	d_{f3}	558	[N/rad]
l_r	0.6	[m]	e_{f1}	-100.9	[N]
l_s	3	[m]	e_{f2}	0	[N]
δ_f^{max}	0.09	[rad]	e_{f3}	100.9	[N]
M_z^{max}	327	[Nm]	d_r	1749.7	[N/rad]
$[\mu_{\delta_f}^{min}, \mu_{\delta_f}^{max}]$	[0.2, 1]		e_r	0	[N]
$[\mu_T^{min}, \mu_T^{max}]$	[0, 0.8]		$\pm\bar{\alpha}_f$	±0.07	[rad]

REFERENCES

[1] M. Spenko, Y. Kuroda, S. Dubowsky, and K. Iagnemma, "Hazard avoidance for high-speed mobile robots in rough terrain," *J. Field Robotics*, vol. 23, no. 5, pp. 311–331, 2006.
[2] A. Terekhov, J.-B. Mouret, and C. Grand, "Stochastic optimization of a chain sliding mode controller for the mobile robot maneuvering," in *Proceedings of IEEE / IROS Int. Conf. on Intelligent Robots and Systems*, 2011, pp. 4360 – 4365.
[3] N. Minoiu Enache, S. Mammar, S. Glaser, and B. Lusetti, "Driver assistance system for lane departure avoidance by steering and differential braking," in *Advances in Automotive Control*, 2010, pp. 471–476.
[4] J. Wang, Q. Wang, L. Jin, and C. Song, "Independent wheel torque control of 4WD electric vehicle for differential drive assisted steering," *Mechatronics*, vol. 21, no. 1, pp. 63 – 76, 2011.
[5] M. Johansson, *Piecewise Linear Control Systems*. Springer, 2002.
[6] A. Hassibi and S. Boyd, "Quadratic stabilization and control of piecewise-linear systems," in *Proceedings of the IEEE American Control Conference, Philadelphia, PA*, 1998, pp. 3659–3664.
[7] L. Rodrigues and J. P. How, "Observer based control of piecewise-affine systems," *Int. J. Control*, vol. 76, no. 5, pp. 459–477, 2003.
[8] D. Bernardini, S. D. Cairano, A. Bemporad, and H. Tseng, "Drive-by-wire vehicle stabilization and yaw regulation: A hybrid model predictive control design," in *Joint 48th IEEE Conference on Decision and Control and 28th Chinese Control Conference, Shanghai, P.R. China*, December 2009, pp. 7621–7626.
[9] A. Benine-Neto and S. Mammar, "Piecewise affine state feedback controller for lane departure avoidance," in *Intelligent Vehicles Symposium (IV), 2011 IEEE*, june 2011, pp. 839 –844.
[10] J. Ackermann, *Robust Control*. London: Springer, 2002.
[11] H. Pacejka, *Tire and Vehicle Dynamics*. Elsevier Butterworth-Heinemann, 2004.
[12] R. Lenain, B. Thuilot, C. Cariou, and P. Martinet, "Mixed kinematic and dynamic sideslip angle observer for accurate control of fast off-road mobile robots." *J. Field Robotics*, vol. 27, p. 181196, 2010.
[13] S. Boyd, L. E. Ghaoui, E. Feron, and V. Balakrishnan, *Linear Matrix Inequalties in System and Control Theory*. SIAM, 1994, ch. 7.
[14] M. Kocvara and M. Stingl, "Pennon: A code for convex nonlinear and semidefinite programming," *Optimization Methods and Software*, vol. 18, no. 3, pp. 317–333, 2003.
[15] M. C. Grant and S. Boyd, "Cvx: Matlab software for disciplined convex programming," http://cvxr.com/cvx/, 2011.
[16] S. Mammar and D. Koenig, "Vehicle handling improvement by active steering," *Vehicle System Dynamics*, vol. 38, no. 3, pp. 211–242, 2002.